JOURNAL OF MATERIALS SCIENCE **20** (1985) 4309–4316

Preparation of porous glass–ceramics of the TiO_2–SiO_2 system

TOSHINORI KOKUBU
Department of Industrial Chemistry, Miyakonojo National College of Technology, Yoshio-cho, Miyakonojo, Miyazaki 885, Japan

MASAYUKI YAMANE
Department of Inorganic Materials, Tokyo Institute of Technology, Ookayama, Meguro-ku, Tokyo 152, Japan

Porous glass–ceramics of the TiO_2–SiO_2 system of high titania content have been prepared by heat treatment and subsequent acid leaching of phase-separated glasses of the TiO_2–SiO_2–Al_2O_3–B_2O_3–CaO–MgO (or –Na_2O) system. The porous glass–ceramics obtained in the study had a surface area of 100 to 300 $m^2 g^{-1}$, with an average pore radius of 3 to 9 nm. The ceramics which contained a large amount of anatase and rutile were expected to be applied in the field of photocatalysts.

1. Introduction

The preparation of porous glasses of high silica content by the extraction of a B_2O_3-rich phase from phase-separated glasses of the borosilicate system was reported for the first time in 1934 [1]. Since then, there have been many papers reporting the preparation of porous glasses by similar techniques [2–8].

The porous glasses prepared via phase separation have a high surface area of 100 to 400 $m^2 g^{-1}$ and have been applied to a variety of fields of engineering, such as support for catalysts [9], adsorbant of chemicals [10, 11] reactive filters for separation and so on [12–15].

On the other hand, a glass of suitable composition can be converted to a glass–ceramic having excellent thermal and mechanical properties by heat treatment above the glass transition temperature. So, it is expected that the combination of both phase-separation and crystallization techniques will allow us to prepare porous glass–ceramics having properties characteristic of crystals precipitated from the phase-separated glass.

In the present study, new porous glass–ceramics of the TiO_2–SiO_2 system with high titania content have been prepared from phase-separated multicomponent glasses of the TiO_2–SiO_2–Al_2O_3–B_2O_3–CaO–MgO and TiO_2–SiO_2–Al_2O_3–B_2O_3–CaO–Na_2O systems.

Since the porous glass–ceramics contain a large amount of anatase and rutile in their skeleton, they are expected to be applied to the same field of functional materials as crystalline titania like photocatalysts [16–25], and gas sensors, in addition to the application to the field of conventional porous glasses.

This paper reports the fabrication method of porous glass–ceramics of high titania content, and some phenomena observed in the phase separation and crystallization process of the glasses.

2. Experimental details

2.1. Preparation of glasses

The experiment was conducted on glasses of two fundamental systems. One was the TiO_2–SiO_2–Al_2O_3–B_2O_3–CaO–MgO system and the other was the TiO_2–SiO_2–Al_2O_3–B_2O_3–CaO–Na_2O system. The glass compositions selected after preliminary study for the detailed investigation are shown in Table I. Raw materials employed were titanium dioxide, anhydrous silicic acid, aluminum oxide, boron trioxide, calcium carbonate, magnesium oxide and anhydrous sodium carbonate, which were all

TABLE I Glass compositions

Sample No.	Composition (mol %)						
	TiO_2	SiO_2	Al_2O_3	B_2O_3	CaO	MgO	Na_2O
1	26.0	26.0	10.0	5.0	28.0	5.0	–
2	26.0	26.0	16.0	5.0	24.5	–	2.5
3	17.0	34.0	13.0	7.0	24.0	5.0	–
4	25.0	31.0	12.5	7.5	22.5	1.5	–

Analar grade reagents. The glass batch was mixed briefly with a porcelain mill and fused at 1673 K for 1 h in a Pt–2%Rh crucible using an electrical furnace. The melt was quenched by pouring into water, by drawing into a fibre or by pressing with two cooling stones into a plate.

2.2. Heat treatment and acid leaching

The heat treatment of the glass for phase separation and crystallization was made at a temperature between 973 and 1123 K for a predetermined period. The brown-coloured transparent glass turned opalescent or opaque by this heat treatment. The phase-separated glass was successively subjected to acid leaching with an HCl solution at 373 K by refluxing for 1 to 12 h. The concentration of HCl was 1 to 4 N for particulate samples of a size between 0.25 and 0.5 mm, and 0.5 N for plate glass of 0.5 mm in thickness. A longer leaching period with more dilute solution for plate glass was adopted to prevent it from fracturing.

By this acid treatment, a phase rich in Al_2O_3–B_2O_3–CaO–MgO (or –Na_2O) phase was leached out, leaving a highly porous skeleton composed of TiO_2 and SiO_2. It was then dried out in a vacuum oven at 383 K. A flow diagram of the process is shown in Fig. 1.

2.3. Chemical analysis

The chemical composition of the titanium-containing porous glass–ceramics was determined by the following methods for respective constituents. SiO_2 was determined by gravimetry and spectroscopy with molybdenum blue. TiO_2 was measured by spectroscopy using diantipyrylmethan. Al_2O_3 was measured by fluorescence spectrometry using Calcon* as fluorescent reagent. B_2O_3 was determined with an ion electrode (made by Toa Electronics Ltd) on a sample dissolved in hydrofluoric acid, by measuring the strength of the BF ion. CaO, MgO and Na_2O were measured by atomic absorption with a Hitachi 207 atomic absorption spectrometer.

2.4. Measurement of the properties of phase-separated glasses and porous glass–ceramics

The detailed investigation on the properties of glass before and after phase separation and crystallization was conducted on Glass No. 4 which was fabricated into a plate very easily.

Differential thermal analysis (DTA) was carried out with a Rigaku Denki 8076 D–1 thermal analyser on a pulverized sample of 53 to 74 μm at a rate of 5 K min^{-1}.

X-ray diffraction study was made on both pulverized and platelet samples with a Shimazu XD 5–A diffractometer using nickel-filtered Cu$K\alpha$ radiation at 30 kV, 20 mA. The pulverized sample had been heated at a constant rate of 5 K min^{-1}, i.e. the same rate as for DTA, to a temperature below or above the respective peaks of the DTA trace, and cooled from there

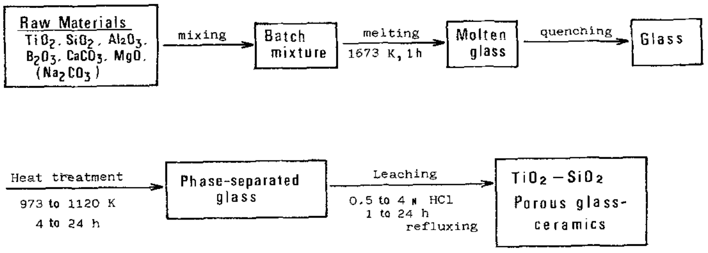

Figure 1 Block diagram for fabricating porous glass–ceramics.

*$HOC_{10}H_6N{:}NC_{10}H_5(OH)\,SO_3Na$ (Indicator for complexometry of Al, Fe, Zr).

as soon as the temperature was attained. The platelet sample had been isothermally treated at 978, 1018, 1033 and 1063 K for various periods of time.

Small-angle X-ray scattering (SAXS) measurements and electron microscopy were also made on the same samples used for X-ray diffraction study. SAXS data were obtained using a Rigaku Denki SAXS system having a Kratky U-slit of 70 μm in width. The incident-beam wavelength was 0.0707 nm, characteristic of zirconium-filtered Mo*Kα* radiation. The intensity of scattered X-rays from a platelet sample of about 1 mm in thickness was measured with a scintilation counter at various angles from 0.05° to 0.65° for 200 sec.

Transmission electron microscopy (TEM) was made by using a JEOL 200 CX at an acceleration voltage of 200 kV.

Specific surface area and the pore-size distribution of the porous glass–ceramics were measured by nitrogen adsorption with a Sorptomatic Series 1800 of Carlo Erba Co. The sample glasses were degassed at 473 K.

3. Results

3.1. DTA, X-ray diffraction, SAXS and TEM

The DTA trace of Glass No. 4 is shown in Fig. 2. The glass transition temperature was observed in the vicinity of 950 K. There were two distinct exothermic peaks at 1008 and 1183 K. The DTA curve of other glasses were all similar to that of No. 4, i.e. there were two distinct exothermic peaks, although the temperatures and the sharpness of the peaks were slightly different.

Fig. 3 shows the powder X-ray diffraction pattern of pulverized samples heated to the temperatures indicated on the inserted DTA trace. It is concluded from Fig. 3 that the first peak at 1008 K may be attributed to the deposition of anatase, the small peak at 1078 K to rutile, and the second distinct peak at 1183 K to the crystallization of $CaAl_2Si_2O_8$. The X-ray diffraction pattern of platelet samples isothermally treated at various temperatures and times are shown in Fig. 4 along with that of untreated glass. A trace of crystallinity was detected in the sample subjected to heat treatment at 978 K up to 36 h, although the temperature was well below the first exothermic peak of the DTA curve. The crystals deposited at 1018 and 1033 K were anatase and rutile, and the amount of the latter increased with increasing heating temperature and time. The deposit of $CaAl_2Si_2O_8$, as well as rutile, was remarkable in the glass held at 1063 K.

The X-ray diffraction pattern of porous glass–ceramics was similar to those of phase-separated glasses before acid treatment, i.e. the crystals were anatase and rutile, as is seen in Fig. 5 where only rutile was observed on the sample heated at 1043 K for 15 h.

Fig. 6 shows a log–log plot of scattering intensity against the scattering vector $K = (4\pi/\lambda)(\sin\theta)$, where λ is the wavelength of the X-rays ($= 0.0707$ nm) and 2θ is the scattering angle. It should be noted that phase separation giving an appreciable amount of scattering had already occurred in the untreated glass. The slope in the Porod region, i.e. crudely $10 > K^{-1} > 1$ (nm), was about -2 for untreated glass and about -3 for all of the heat-treated samples. This indicates

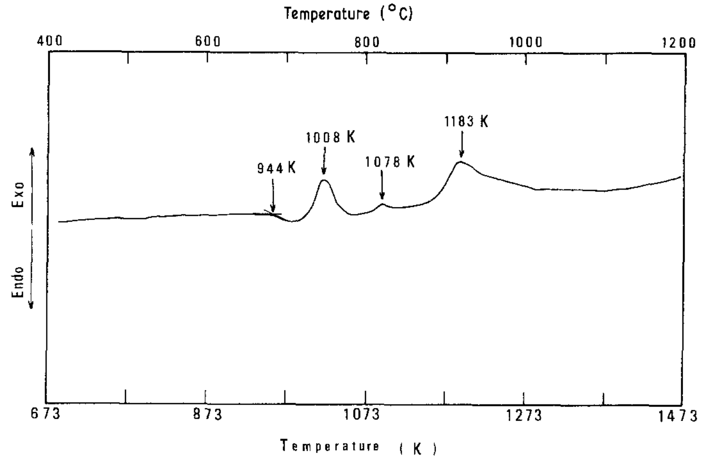

Figure 2 DTA trace of Glass No. 4.

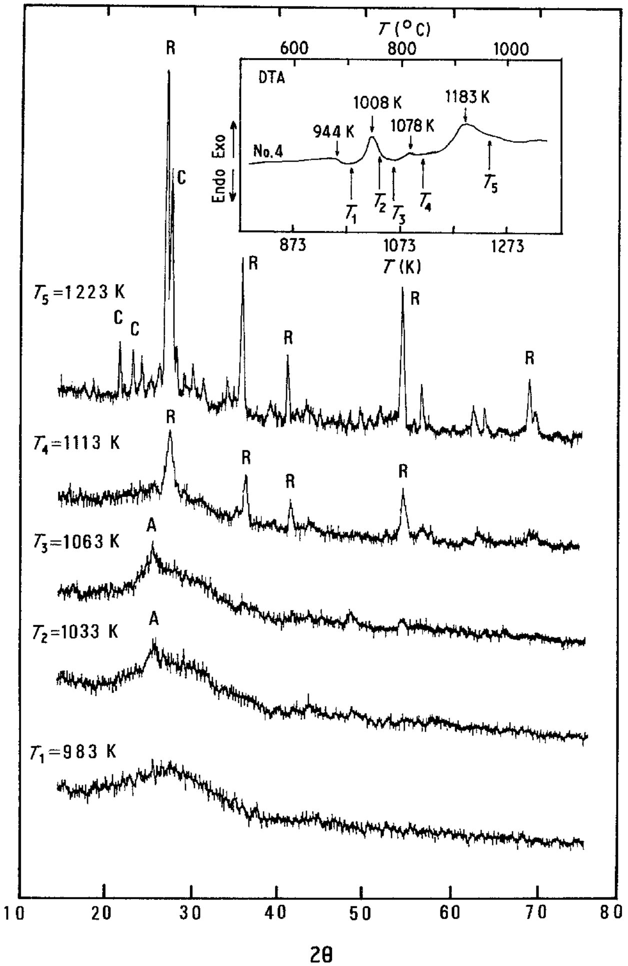

Figure 3 Powder X-ray diffraction pattern of Glass No. 4 heated at 5 K min^{-1} to temperatures shown on the DTA trace (insert). (A) anatase, (R) rutile, (C) $CaAl_2Si_2O_8$.

that the ambiguous phase boundary in untreated glass became clear with heat treatment [26].

Fig. 7 shows electron micrographs of samples after various heat treatments. The interconnected structure of two separated phases in the untreated glass developed remarkably by heat treatment at 978 K for 12 h. The size of cross-section of one of the phases is estimated to be 5 to 10 nm in diameter. The size of the separated phases became slightly larger after treatment at higher temperatures (1018, 1033 K) where the deposition of crystals was appreciable.

3.2. Chemical composition of porous glass

The glass held at 978 K for 36 h became porous by acid treatment, although the glass did not remain monolithic. The glass heat-treated at a temperature where the deposition of anatase and rutile had been observed became a monolithic porous body with acid treatment, while the one heated at a higher temperature (where $CaAl_2Si_2O_8$ had deposited) dissolved completely in a hot acid solution.

The chemical compositions of some porous glass–ceramics are shown in Table II. Compared with the values of the original glasses in Table I, the decrease in the amounts of B_2O_3, CaO, MgO, Al_2O_3 and Na_2O is remarkable. Although the composition of the final product was dependent on leaching conditions, the skeleton mostly consisted of titania and silica.

3.3. Specific surface area and pore-size distribution

The specific surface area of the porous glass–ceramics prepared by heat treatment at various temperatures and times are plotted in Figs. 8 and 9. It is concluded that the specific surface area decreased with a rise in temperature or prolonged heating time, due to coarsening of the separated phases. These phenomena agree with

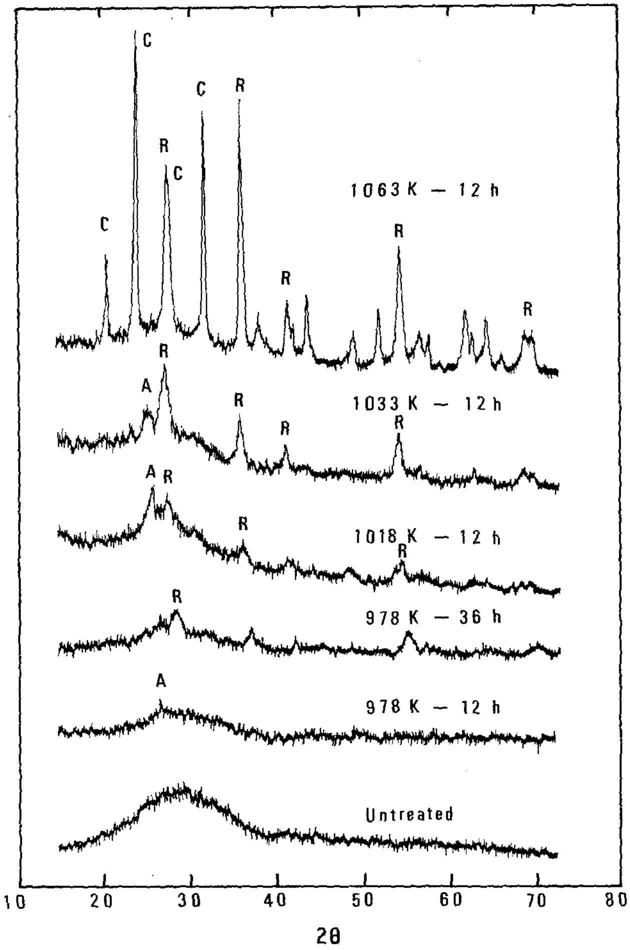

Figure 4 X-ray diffraction pattern of isothermally heated Glass No. 4. (A) anatase, (R) rutile, (C) $CaAl_2Si_2O_8$.

the results of SAXS measurement and electron microscopy. The curves shown in Fig. 10 are the pore-size distribution in the porous glass–ceramics prepared from Glass No. 4. The average pore radius was in the range 3 to 9 nm, and became large with an increase in the temperature of heat treatment. Although it is not shown in Fig. 10, a glass–ceramic

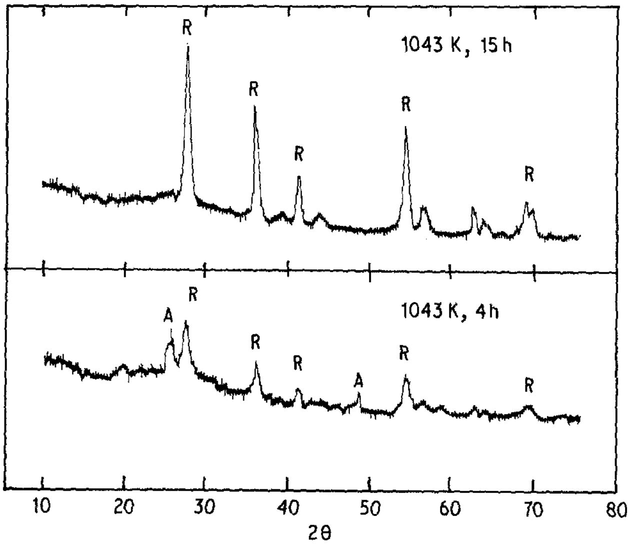

Figure 5 X-ray diffraction pattern of porous glass–ceramics prepared from Glass No. 4. (A) anatase, (R) rutile.

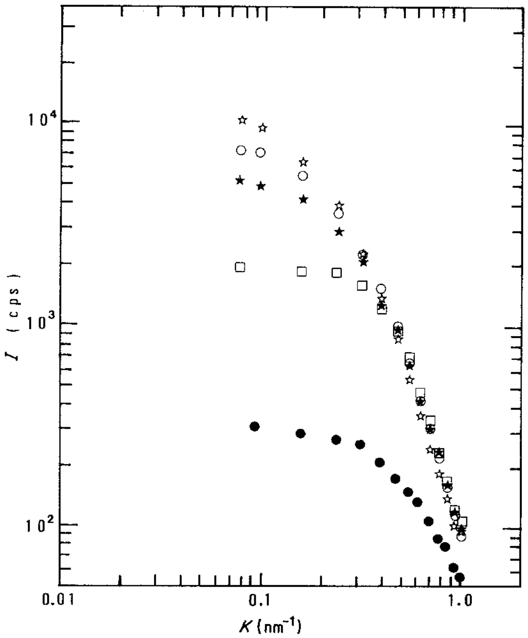

Figure 6 Development of scattering profile with heat treatment. (●) untreated glass; (□) 978 K, 12 h; (○) 978 K, 36 h; (★) 1081 K, 12 h; (☆) 1033 K, 12 h.

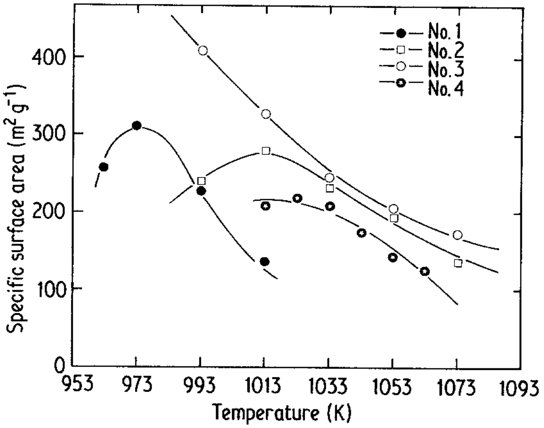

Figure 8 Specific surface area of porous glass–ceramics obtained by heat treatment at various temperatures for 15 h.

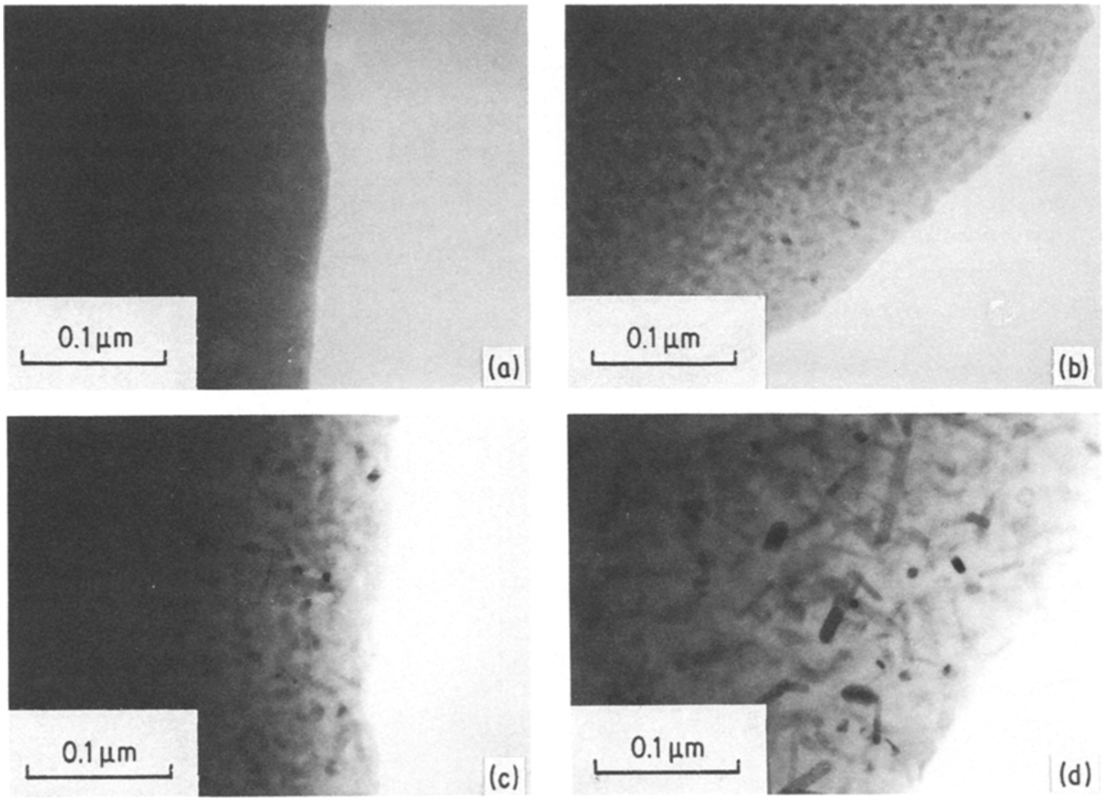

Figure 7 Transmission electron micrographs of phase-separated glasses: (a) untreated; (b) 978 K, 12 h; (c) 1018 K, 12 h; (d) 1033 K, 12 h.

TABLE II Chemical compositions of porous glass–ceramics

Sample No.	Acid treatment	Composition (mol %)					
		TiO_2	SiO_2	Al_2O_3	B_2O_3	CaO	MgO
1	3 N HCl, 4 h	49.5	50.2	0.3	0.0	0.0	0.0
3	3 N HCl, 4 h	37.5	62.4	0.1	0.0	0.0	0.0
4 (plate)	0.5 N HCl, 12 h	45.7	52.6	1.2	0.0	0.3	0.2

having pores as large as 15 nm could be prepared.

4. Discussion

4.1. Development of phase separation and crystallization

It was deduced from SAXS measurement and TEM that phase separation had already occurred in the untreated glass which was obtained by the simple quenching of a melt. The slope of the SAXS intensity in the Porod region of the untreated glass was about -2, which was characteristic of a system containing an ambiguous phase boundary between two phases [26]. Therefore, the phase separation of the glass of the present study is considered to begin with spinodal decomposition, although detailed investigation is necessary for confirmation of this.

The development of phase separation by heat treatment at a temperature above T_g is clear from Figs. 6 and 7. The pattern of development of the SAXS curves with heat treatment is similar to the one representing growth in the size of a fixed number of scatterers [26]. The result of chemical analysis suggests that the separation proceeded in the direction of forming phases rich in TiO_2–SiO_2 and B_2O_3–Al_2O_3–CaO.

It should be noted that no evidence of a second separation into a TiO_2–SiO_2-rich phase could be detected, despite of the existence of a stable two-liquids region in the phase diagram of this system [27].

It is also noteworthy that only a trace of crystallinity was detected in the sample heated to 1063 K, which was well above the first peak of the DTA plot. Since the simple coarsening of a skeletal structure would not give such a distinct exothermic peak, the phenomenon must be attributed to the minuteness of the size of anatase which was the only crystal detected at that temperature. Another possibility for giving a sharp exothermic peak would be the development of a second phase separation in the glassy TiO_2–SiO_2 phase, which must be confirmed by further investigation.

4.2. Comparison of porous glass–ceramics with other titania-containing materials

Since the porous glass–ceramic obtained in this study contains a large amount of rutile and anatase, it can be applied as a photocatalyst for various reactions such as the decomposition of water to produce hydrogen, reduction of CO_2,

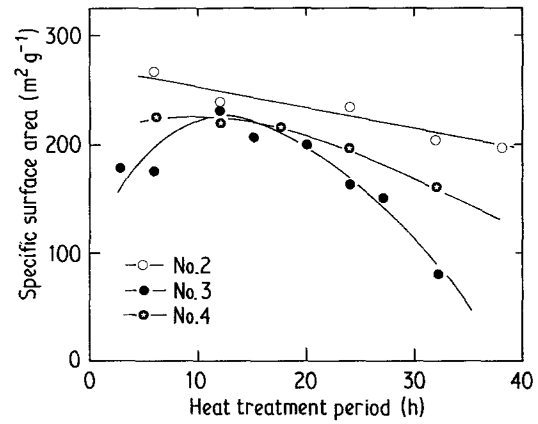

Figure 9 Change in specific surface area with heat treatment at 1033 K.

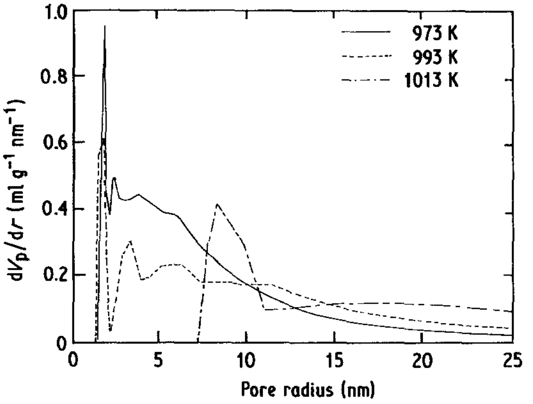

Figure 10 Pore-size distribution in porous glass–ceramics prepared by the acid leaching of heat-treated Glass No. 1 at 973, 993, and 1013 K for 15 h.

fixing of N_2, and decomposition of acetic acid to yield CH_4 and CO_2.

The advantage of the porous glass–ceramic as a photocatalyst will be its high surface area available for supporting platinum, rhodium, NiO etc., which remarkably improves the catalytic efficiency.

The surface area of 100 to 300 $m^2 g^{-1}$ obtained for the porous glass–ceramic of this study was comparable to that of porous TiO_2 prepared by a sol–gel process from $TiCl_4$ [18], and obviously much higher than that of TiO_2 powder or sintered polycrystalline TiO_2. Moreover, the surface area of the porous glass–ceramic can be controlled by selecting the temperature of heat treatment, which is an advantage over porous TiO_2.

The other advantage of a porous glass–ceramic may be the possible variety of its shape. It can be supplied in the form of a powder, fibre or plate according to the purpose for which it is to be used. It also has the advantage that the proportion of anatase to rutile can be controlled by selecting the temperature of heat treatment, so that the band gap may be adjusted.

Acknowledgements

The authors thank S. Sakurada and T. Isoda of the Central Research Laboratory of Toa Nenryo Kogyo Co Ltd for measurements of pore size distribution, X-ray fluorescence analysis and analytical electron microscopy.

References

1. H. P. HOOD *et al.*, US Patent 2 106 774 (1934).
2. C. J. PLANK and N. J. WOODBURY, US Patent 2 472 490 (1949).
3. E. M. RABINOVICH, *J. Mater. Sci.* **15** (1980) 2027.
4. M. A. RES, J. T. FOURTE, R. W. WHITE and J. BENDNARIK, *J. Amer. Ceram. Soc.* **65** (1982) 184.
5. J. J. HAMMEL and TIES ALLERSMA, US Patent 3 843 341 (1974).
6. R. MADDISON and T. W. McMILLAN, *Glass Technol.* **21** (1980) 297.
7. T. NAKAJIMA and Y. KUROKI, *Nippon Kagakukai Schi* **8** (1981) 1231.
8. J. F. RANDNARIC, M. A. RES and R. W. WHITE, *Glass Technol.* **24** (1983) 122.
9. S. HIRAI, A. MORIKAWA, Y. ISHINAGA, K. OTUKA and Y. WADA, *Bull. Chem. Soc. Jpn.* **50** (1977) 3411.
10. W. HALLER, US Patent 3 549 524 (1970).
11. *Idem*, US Patent 3 758 284 (1973).
12. T. H. ELMER, *Amer. Ceram. Soc. Bull.* **57** (1978) 1051.
13. F. E. LITTMAN and G. A. CROOPNIK, US Office Saline Water Research and Development Progress Report No. 720 (1971).
14. R. SCHNABEL *et al.*, *Desalination* **24** (1978) 249.
15. H. V. BAEYER *et al.*, *Trans. Amer. Soc. Artificial Internal Organ* **26** (1980) 309.
16. A. FUJISHIMA and K. HONDA, *Bull. Chem. Soc. Jpn.* **44** (1971) 1148.
17. *Idem, Nature* **238** (1972) 37.
18. L. KRUZYNSKI, H. D. GESSER, C. W. TURNER and E. A. SPEERS, *ibid.* **291** (1981) 399.
19. T. KAWAI and T. SAKATA, *ibid.* **286** (1980) 474.
20. *Idem, J. Chem. Soc. Chem. Commun.* (1980) 694.
21. S. SATO and J. M. WHITE, *J. Amer. Chem. Soc.* **102** (1980) 7206.
22. M. FUJIWARA, Y. SATOH and T. OSA, *Nature* **293** (1981) 206.
23. B. KRAUETLER and A. J. BARD, *J. Amer. Chem. Soc.* **99** (1978) 7729.
24. *Idem, ibid.* **100** (1978) 2239.
25. *Idem, ibid.* **100** (1978) 5985.
26. D. W. SHAEFER and K. D. KEEFER, "Better Ceramics Through Chemistry", edited by C. J. Brinker, D. E. Clark and D. R. Ulrich (North-Holland, 1984) p. 1.
27. R. C. DEVRIES, R. ROY and E. F. OSBORN, *Trans. Brit. Ceram. Soc.* **53** (1954) 531.
28. L. KRUZYNSKI *et al.*, *Nature* **291** (1981) 399.

Received 12 November
and accepted 28 November 1984